

# SCIENTIFIC REPORTS

OPEN

## Super Stable Ferroelectrics with High Curie Point

Zhipeng Gao<sup>1,2</sup>, Chengjia Lu<sup>1</sup>, Yuhang Wang<sup>1</sup>, Sinuo Yang<sup>3</sup>, Yuying Yu<sup>1</sup> & Hongliang He<sup>1</sup>

Received: 26 January 2016

Accepted: 21 March 2016

Published: 07 April 2016

Ferroelectric materials are of great importance in the sensing technology due to the piezoelectric properties. Thermal depoling behavior of ferroelectrics determines the upper temperature limit of their application. So far, there is no piezoelectric material working above 800 °C available. Here, we show  $\text{Nd}_2\text{Ti}_2\text{O}_7$  with a perovskite-like layered structure has good resistance to thermal depoling up to 1400 °C. Its stable behavior is because the material has only 180° ferroelectric domains, complex structure change at Curie point ( $T_c$ ) and their sintering temperature is below their  $T_c$ , which avoided the internal stresses produced by the unit cell volume change at  $T_c$ . The phase transition at  $T_c$  shows a first order behavior which involving the tilting and rotation of the octahedron. The Curie – Weiss temperature is calculated, which might explain why the thermal depoling starts at about 1400 °C.

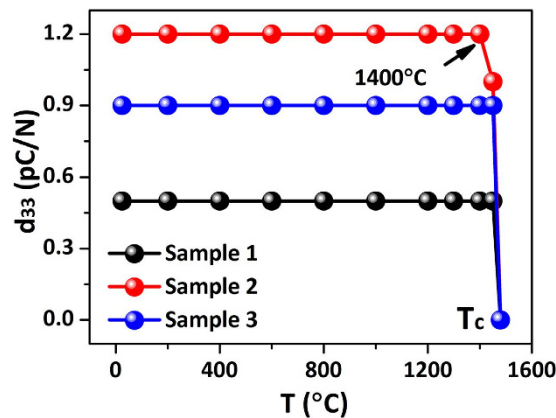
High-temperature piezoelectric sensing technology is of major importance for the chemical and material processing as well as automotive, aerospace, and power generating industries<sup>1,2</sup>. The commercial materials used for high temperature applications such as tourmaline ( $d_{33} \sim 1.5$  pC/N) can only work until 650 °C<sup>1,3–5</sup>. Some ferroelectrics are potential for the high temperature applications due to their high Curie point ( $T_c$ ), such as Aurivillius phase ferroelectrics<sup>6–8</sup>,  $\text{Bi}_{0.5}\text{Na}_{0.5}\text{TiO}_3$ -based ferroelectrics<sup>9–11</sup>, etc. However, all of them could not be used above 700 °C due to their thermal depoling behaviors<sup>6,7</sup>. The thermal depoling behaviors of ferroelectrics determine the upper temperature limit of their application as piezoelectrics. Thermal depoling is related to many factors, such as the phase transitions, ferroelectric domain structure, defects and internal mechanical stress<sup>7,8,12–14</sup>. For lead zirconate titanate ceramics, the internal stress and the non-180° domains reduced the thermal stability of their piezoelectric properties<sup>12</sup>. In the barium titanate system and  $(1-x)(\text{BiScO}_3)-x(\text{PbTiO}_3)$  compounds, the internal stress can seriously affect the thermal depoling stability<sup>14,15</sup>. Defects in ferroelectrics can interact with domain walls and inhibit their movement at room temperature. However they can be thermally decoupled, which can produce thermal depoling<sup>13</sup>. In Aurivillius phase ferroelectrics, the non-180° domains could reduce the thermal stability<sup>7,8</sup>.

The ferroelectrics with perovskite-like layer structure (PLS) ferroelectrics show high Curie point ( $>1000$  °C)<sup>16–19</sup>. In recent years, many investigations have focused on their potential to be used in high temperature piezoelectric sensor applications<sup>18–21</sup>. However, there is very limited information on the thermal depoling of PLS phase materials. In the present study, PLS ferroelectric ceramic,  $\text{Nd}_2\text{Ti}_2\text{O}_7$ , was investigated and surprisingly it shows a super stable thermal depoling behavior up to 1400 °C. This opens a door for the development of new ferroelectrics for high temperature applications.

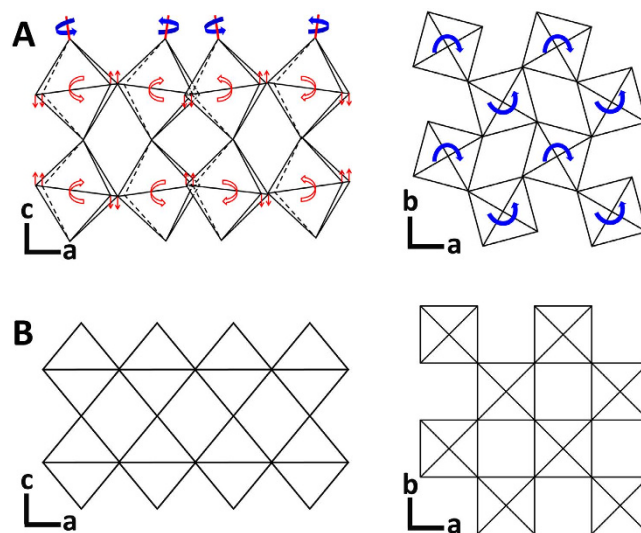
### Results and Discussions

Fig. 1A shows the thermal depoling behavior of  $\text{Nd}_2\text{Ti}_2\text{O}_7$  ceramics, in which the piezoelectric constant  $d_{33}$ , measured at room temperature, are plotted against the annealing temperature. The values of  $d_{33}$  of  $\text{Nd}_2\text{Ti}_2\text{O}_7$  samples (1–3) were measured as 0.5, 1.2, and 0.9 pC/N, respectively. The  $d_{33}$  value is very stable up to 1400 °C and drop to zero at about 1480 °C, which is the Curie temperature of  $\text{Nd}_2\text{Ti}_2\text{O}_7$ . The variation of the  $d_{33}$  value is mainly due to the different poling conditions of these three samples. The sample 1, 2 and 3 were poled under the electric field as 20, 27 and 24 kV/mm, respectively. The difference of the poling electrical field is because of the different breakdown field of each sample. During the experiment, the thin ceramic sample was poled in the silicone oil at a temperature of 120 °C under an electric field. We increased the electrical field gradually from 10 kV/mm until the sample was electric breakdown. Therefore, the breakdown field of each sample decides the poling field, which can affect the piezoelectric activity. Compared to other ferroelectric compounds, the thermal depoling temperature of  $\text{Nd}_2\text{Ti}_2\text{O}_7$  is about 600 °C, 800 °C and 1000 °C higher than the values of Aurivillius phases,  $\text{Bi}_{0.5}\text{Na}_{0.5}\text{TiO}_3$ -based compounds (BNT), and  $\text{Pb}(\text{Zr,Ti})\text{O}_3$  compounds (PZT), respectively<sup>6–8,13,22–24</sup>. This makes  $\text{Nd}_2\text{Ti}_2\text{O}_7$  a great

<sup>1</sup>National Key Laboratory of Shock Wave and Detonation Physics, Institute of Fluid Physics, China Academy of Engineering Physics, Mianyang 621900, China. <sup>2</sup>Southwest University of Science and Technology, Mianyang 621010, China. <sup>3</sup>Liansu Ltd., 777 Hongqi road, Jiamusi 154002, China. Correspondence and requests for materials should be addressed to Z.G. (email: z.p.gao@foxmail.com)



**Figure 1.** Effect of thermal annealing on piezoelectric properties ( $d_{33}$ ).



**Figure 2.** The structure of  $\text{Nd}_2\text{Ti}_2\text{O}_7$  projected along the b- and c-axis for (A) ferroelectric phase ( $P2_1$ ) and (B) paraelectric phase ( $Cmcm$ ).

candidate for the high temperature sensor applications, considering its  $d_{33}$  is acceptable, which is higher than the  $d_{33}$  of commercial piezoelectrics - tourmaline. Actually, this PLS ferroelectric material,  $\text{Nd}_2\text{Ti}_2\text{O}_7$ , exhibits the highest temperature stability of piezoelectric properties among all known ferroelectrics so far as we know. The fact that PLS ferroelectrics only have  $180^\circ$  domains might explain the stability of these compounds.  $\text{Nd}_2\text{Ti}_2\text{O}_7$  has a monoclinic ferroelectric structure with  $P2_1$  space group, and the lattice parameters is  $(a, b, c, \beta) = (13.020 \text{ \AA}, 5.480 \text{ \AA}, 7.680 \text{ \AA}, 98.3^\circ)$  as shown in Fig. 2A<sup>21,25–29</sup>. The paraelectric phase of  $\text{Nd}_2\text{Ti}_2\text{O}_7$ , above the  $T_c$ , is orthorhombic lattice with the space group of  $Cmcm$ <sup>27,28</sup>, shown in Fig. 2B. The ferroelectric spontaneous polarization ( $P_s$ ) is induced by the rotation of the  $\text{TiO}_6$  octahedron around c-axis (blue arrow) and tilt around b-axis (red arrow), shown in Fig. 2A, which lead the  $P_s$  only in b-axis, producing  $180^\circ$  domains. In ferroelectric materials, the switching of non- $180^\circ$  domains produces a shape change<sup>30,31</sup>. This can lead to large mechanical internal stress in poled materials. These internal stresses combined with thermal activation can produce thermal depoling. These effects are absent in materials with only  $180^\circ$  switching. Additionally, the ferroelectric to paraelectric phase transition of  $\text{Nd}_2\text{Ti}_2\text{O}_7$  involves all of the ions, from the  $\text{TiO}_6$  octahedron rotation and tilt. This characteristic might be another reason for its good stability and high  $T_c$ , due to that the complex structure change increase activation energy of phase transition. Furthermore, the sintering temperature of  $\text{Nd}_2\text{Ti}_2\text{O}_7$  ceramic ( $1350^\circ\text{C}$ ), which is lower than the  $T_c$  ( $1481^\circ\text{C}$ ), can reduce internal stress and increase thermal stability in this ferroelectric ceramic. Because sintering ceramics below its  $T_c$  can avoid the volume change associated with the Curie transition temperature on cooling from the sintering temperature.

Figure 3A shows the spontaneous polarization ( $P_s$ ) value of  $\text{Nd}_2\text{Ti}_2\text{O}_7$  based on the atomic displacements. Ionic displacements along the b-axis from the corresponding positions in the paraelectric structure produce the ferroelectric spontaneous polarization. Displacements along the a- and c- axes are cancelled due to the presence of centro-symmetric centers, which are therefore do not contribute to the total  $P_s$ . Based on the ionic displacements, the total  $P_s$  of ferroelectric  $\text{Nd}_2\text{Ti}_2\text{O}_7$  was calculated using Shimakawa's model<sup>8,32</sup>:

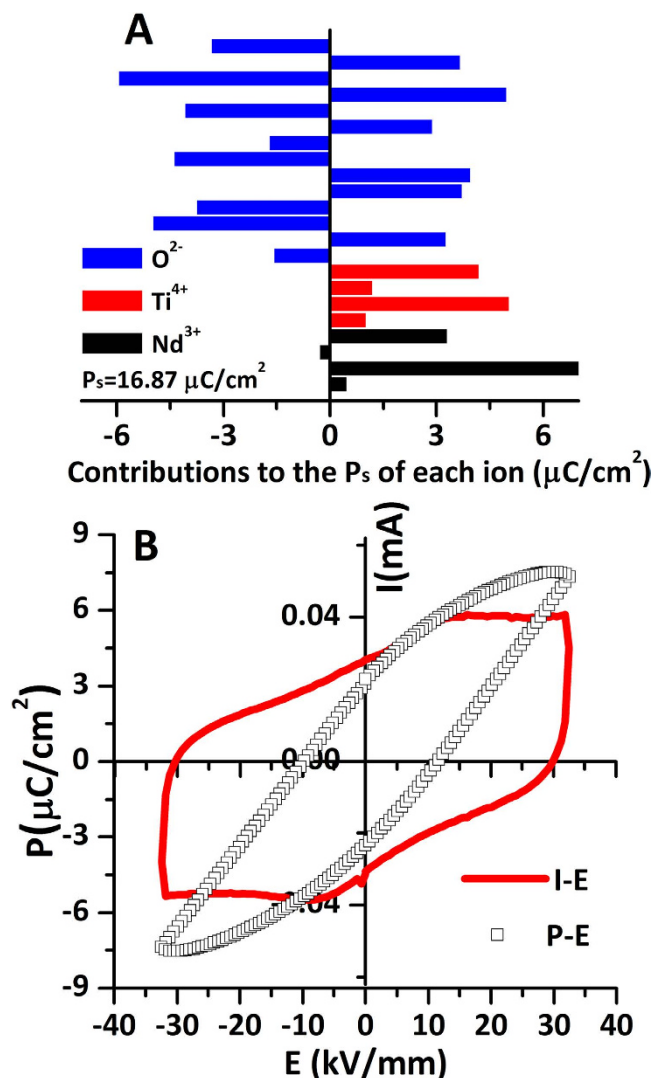


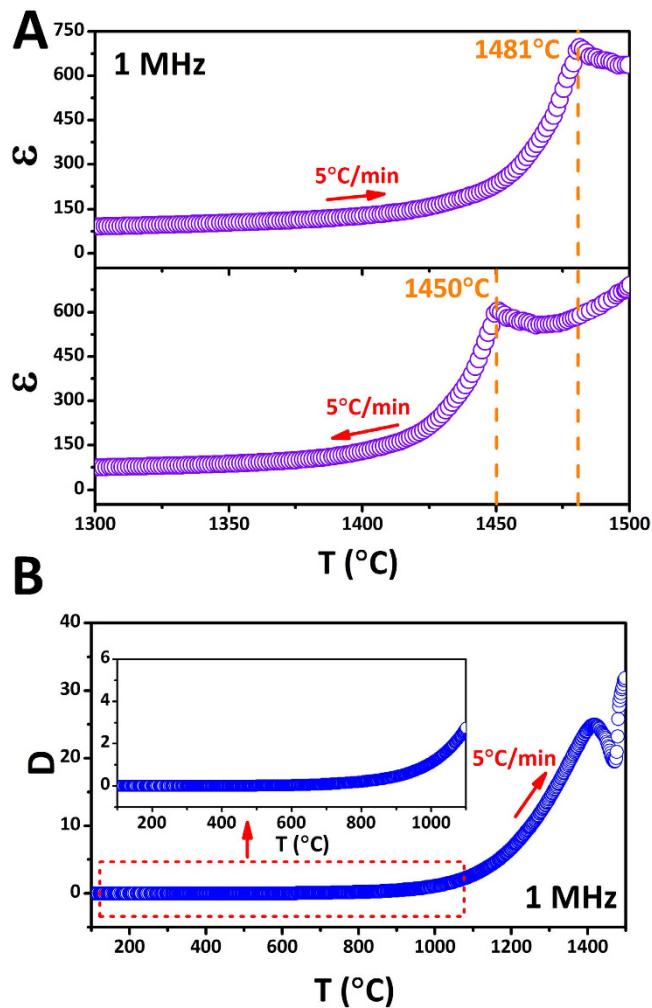
**Figure 3.** (A) Ionic contribution to total spontaneous polarization ( $P_s$ ) of each ion of  $\text{Nd}_2\text{Ti}_2\text{O}_7$ . (B) The polarization – electric field plot (P–E) and current – electric field plot (I–E) measured at a frequency of 5 Hz.

$$P_s = \sum_i \frac{m_i \Delta x_i Q_{ie}}{V} \quad (1)$$

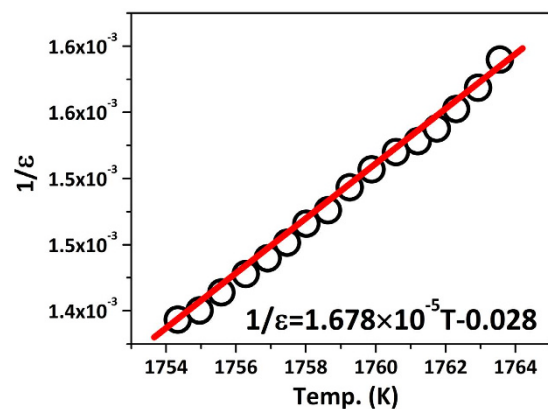
where  $m_i$  is the site multiplicity and  $\Delta x_i$  is the atomic displacement along the  $c$ -axis,  $Q_{ie}$  is the ionic charge of the ion, and  $V$  is the volume of the unit cell. According to the crystal structure parameters of  $\text{Nd}_2\text{Ti}_2\text{O}_7$  reported on the single crystals<sup>23–29</sup>, the ionic contributions to the total  $P_s$  are presented in Fig. 3A, and the total  $P_s$  is calculated as  $16.87 \mu\text{C}/\text{cm}^2$  at room temperature. Figure 3B shows the polarization – electric field plot (P–E) and current – electric field plot (I–E). From the un-saturated P–E plot, the  $P_r$  value is about  $4.2 \mu\text{C}/\text{cm}^2$ , which is much smaller than the value calculated. The coercive field is about  $10 \text{ kV}/\text{mm}$ .

Figure 4A shows dielectric constant ( $\epsilon$ ) of  $\text{Nd}_2\text{Ti}_2\text{O}_7$  ceramic as function of temperature at 1 MHz measured at heating and cooling processes at a rate of  $5^\circ\text{C}/\text{min}$ . Typically, the dielectric constant peaks indicate the ferroelectric to paraelectric phase transitions (Curie point,  $T_c$ ). The  $T_c$  at heating process is observed as  $1481^\circ\text{C}$  which is in a good agreement with the literatures<sup>21,22,33</sup>. However, the  $T_c$  for the cooling process was different from heating which is  $1450^\circ\text{C}$ . The difference between heating and cooling suggests the ferroelectric to paraelectric transition of  $\text{Nd}_2\text{Ti}_2\text{O}_7$  has thermal hysteresis, which means this is a first order transition. This is also supported by the Curie - Weiss fitting. The function of  $1/\epsilon$  to temperature above  $T_c$  is shown in Fig. 5 according to the equations 2 and 3, where  $C$  is a material-specific Curie constant,  $T$  is the absolute temperature, and  $T_0$  is the Curie - Weiss temperature<sup>31</sup>.

$$\epsilon = \frac{C}{T - T_0} \quad (2)$$



**Figure 4.** (A) Temperature dependence of the dielectric constant of  $\text{Nd}_2\text{Ti}_2\text{O}_7$  at 1 MHz in the processes of heating and cooling. (B) The loss ( $\tan\theta$ ) measured from 100 °C to 1500 °C at the frequency of 1 MHz, and the insert figure is the enlargement of range from 100 °C to 1100 °C.



**Figure 5.** Curie-Weiss fitting for the dielectric constant above the  $T_c$  for  $\text{Nd}_2\text{Ti}_2\text{O}_7$ .

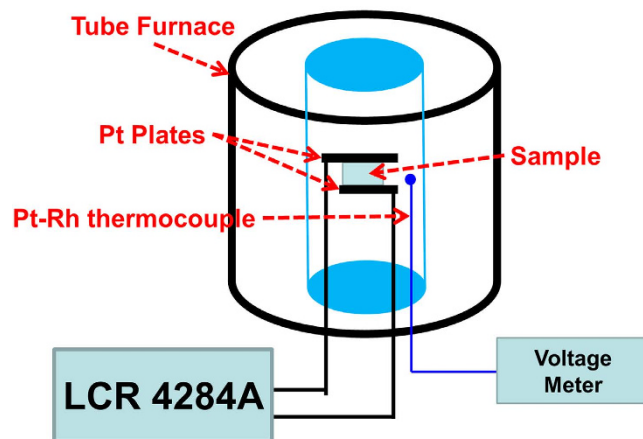


**Figure 6.** The experimental set up used to measure permittivity and loss at high temperature.

$$\frac{1}{\varepsilon} = \frac{T}{C} - \frac{T_0}{C} \quad (3)$$

For  $\text{Nd}_2\text{Ti}_2\text{O}_7$ , the slope of the fitting is  $1.678 \times 10^{-5}$ , which is  $1/C$ , and the intercept is the  $T_0/C$  measured as 0.028, and the  $T_0$  is estimated as  $1395^\circ\text{C}$ , lower than  $T_c$  in heating process. The  $T_0$  indicates the temperature point, at which the  $P_s$  starts going down, and this result might explain why the thermal depoling of  $\text{Nd}_2\text{Ti}_2\text{O}_7$  start at about  $1400^\circ\text{C}$ . The loss ( $\tan\theta$ ) at the heating process was shown in Fig. 4B and the insert figure is the enlargement of range from  $100^\circ\text{C}$  to  $1100^\circ\text{C}$ . The loss increase with the temperature increasing, and there is a broad peak just below the  $T_c$ , which can be attributed to ferroelectric domain wall movement. The loss below  $1000^\circ\text{C}$  is small and this is helpful to develop the piezoelectric applications in the future.

In summary, perovskite-like layer structured ferroelectric,  $\text{Nd}_2\text{Ti}_2\text{O}_7$ , has super high Curie points and stable piezoelectric properties. The stability of the piezoelectric properties can be explained by their stable ferroelectric domain structure, which consists of only  $180^\circ$  domains; the complex structure at  $T_c$ ; and the fact that their sintering temperatures are below  $T_c$ , which avoids the internal strain produced by the volume change at  $T_c$ . The thermal depoling of  $\text{Nd}_2\text{Ti}_2\text{O}_7$  starts at about  $1400^\circ\text{C}$ , which is the Curie - Weiss temperature, at which the  $P_s$  begin disappearing. This material has the potential to produce a step forward in the maximum operating temperature of ferroelectric/piezoelectric ceramics to  $>1000^\circ\text{C}$ .

**Experiment Procedure.** The starting materials were  $\text{Nd}_2\text{O}_3$  (99.9% purity, Alfa Aesar) and  $\text{TiO}_2$  (99.95% purity, Alfa Aesar). The calcination conditions were  $1250^\circ\text{C}$  for 4 h for powder synthesis. The ceramic was fabricated in a spark plasma sintering furnace (HPD 25/1, FCT Systems, Germany) using a two-step method<sup>5,6</sup>. The  $\text{Nd}_2\text{Ti}_2\text{O}_7$  powder was sintered at  $1150^\circ\text{C}$  under 80 MPa for 3 min in a 20 mm-diameter graphite die firstly. Then the sintered ceramics were sintered at  $1350^\circ\text{C}$  under 30 MPa for 5 min in a die with 30 mm diameter. X-ray diffraction (XRD, Siemens D5000, Karlsruhe, Germany) patterns was used to detect the phase of the ceramics. Electrodes were fabricated with fired-on platinum paste (Gwent Electronic Materials Ltd, C2011004D5) for electrical properties measurements. The temperature dependence of dielectric constant and loss was measured using a LCR meter (Agilent 4284A) connected to a tube furnace as shown in Fig. 6. The P-E and I-E loops were collected on the ferroelectric test module (TF Analyzer 2000 FE-module, aixACCT, Aachen, Germany). Samples for piezoelectric measurements were poled under various DC electric fields (20–30 kV/mm) in silicone oil at a temperature of  $120^\circ\text{C}$ . We increased the electrical field gradually from 10 kV/mm until the sample was electrical breakdown to obtain high  $d_{33}$ . Then their piezoelectric constant  $d_{33}$  was measured using a quasi-static  $d_{33}$  meter (CAS, ZJ- 3B) with the instrument precision of 0.1 pC/N<sup>17</sup>. To confirm the small  $d_{33}$  is not an experiment error, both sides of the sample was measured and the  $d_{33}$  are positive and negative on each side with the same absolute values. The  $d_{33}$  is zero on the un-poled samples as measured. The thermal depoling behavior was investigated by holding the samples at a fixed temperature for 4 hours, then measuring their piezoelectric constant after cooling.

## References

1. Damjanovic, D. Materials for high temperature piezoelectric transducers. *Curr. Opin. Solid St. M.* **3**, 469–473 (1998).
2. Turner, R. C., Fuijierer, P. A., Newnham, R. E. & Shrout, T. R. Materials for high - temperature acoustic and vibration sensors - a review. *Appl. Acoust.* **41**, 299–324 (1994).
3. Shekhar Pandey, C., Jodlauk, S. & Schreuer, J. Correlation between dielectric properties and chemical composition of the tourmaline single crystals. *Appl. Phys. Lett.* **99**, 3 (2011).
4. Zhang, S. J. *et al.* High-temperature piezoelectric single crystal  $\text{ReCa}_4\text{O}(\text{BO}_3)_3$  for sensor applications. *IEEE Trans. Ultrason. Ferroelectr. Freq. Control.* **55**, 2703–2708 (2008).
5. Tressler, J. F., Alkoy, S. & Newnham, R. Piezoelectric sensors and sensor materials. *J. Electroceram.* **2**, 257–272 (1998).
6. Yan, H. *et al.* Effect of texture on dielectric properties and thermal depoling of  $\text{Bi}_4\text{Ti}_3\text{O}_{12}$  ferroelectric ceramics. *J. Appl. Phys.* **100**, 076103 (2006).

7. Yan, H. Zhang, H., Reece, M. & Dong, X. Thermal depoling of high curie point aurivillius phase ferroelectric ceramics. *Appl. Phys. Lett.* **87**, 082911 (2005).
8. Yan, H. *et al.* A lead - free high curie point ferroelectric ceramic,  $\text{CaBi}_2\text{Nb}_2\text{O}_9$ . *Adv. Mater.* **17**, 5 (2005).
9. Kruzina, T. V., Sidak, V. M., Trubitsyn, M. P., Popov, S. A. & Suchanicz, J. Thermal treatment and dielectric properties of  $\text{Na}_{0.3}\text{Bi}_{0.5}\text{TiO}_3$  single crystal. *Ferroelectrics* **462**, 140 (2014).
10. Dorcet, V., Trolliard, G. & Boullay, P. Reinvestigation of phase transitions in  $\text{Na}_{0.5}\text{Bi}_{0.5}\text{TiO}_3$  by TEM. Part I: First order rhombohedral to orthorhombic phase transition. *Chem. Mater.* **20**, 5061–5073 (2008).
11. Trolliard, G. & Dorcet, V. Reinvestigation of phase transitions in  $\text{Na}_{0.5}\text{Bi}_{0.5}\text{TiO}_3$  by TEM. Part II: Second order orthorhombic to tetragonal phase transition. *Chem. Mater.* **20**, 5074–5082 (2008).
12. Wan, S. & Bowman, K. Thermal depoling effects on anisotropy of lead zirconate titanate materials. *J. Am. Ceram. Soc.* **81**, 2717–2720 (1998).
13. Zeng, T., Yan, H. X. & Reece, M. J. Effect of point defects on thermal depoling behavior of bismuth layer-structured ferroelectric ceramics. *J. Appl. Phys.* **108**, 9 (2010).
14. Hao, J., Bai, W., Li, W. & Zhai, J. Correlation between the microstructure and electrical properties in high-performance  $(\text{Ba}_{0.85}\text{Ca}_{0.15})(\text{Zr}_{0.1}\text{Ti}_{0.9})\text{O}_3$  lead-free piezoelectric ceramics. *J. Am. Ceram. Soc.* **95**, 6 (2012).
15. Chen, S., Dong, X. L., Mao, C. L. & Cao, F. Thermal stability of  $(1-x)\text{BiScO}_3-x\text{PbTiO}_3$  piezoelectric ceramics for high-temperature sensor applications. *J. Am. Ceram. Soc.* **89**, 3270–3272, (2006).
16. Nanamats, S., Kimura, M., Doi, K. & Takahashi, M. Ferroelectric properties of  $\text{Sr}_2\text{Nb}_2\text{O}_7$  single crystal. *J. Phys. Soc. Jpn.* **30**, 300 (1971).
17. Nanamats, S., Kimura, M., Doi, K., Matsushita, S. & Yamada, N. A new ferroelectric:  $\text{La}_2\text{Ti}_2\text{O}_7$ . *Ferroelectric.* **8**, 1, 511–513 (1974).
18. Ning, H. P., Yan, H. X. & Reece, M. J. Piezoelectric strontium niobate and calcium niobate ceramics with super-high curie points. *J. Am. Ceram. Soc.* **93**, 1409–1413 (2010).
19. Gao, Z. P., Yan, H. X., Ning, H. P. & Reece, M. J. Ferroelectricity of  $\text{Pr}_2\text{Ti}_2\text{O}_7$  ceramics with super-high curie point. *Adv. Appl. Ceram.* **112**(2), 69–74 (2013).
20. Gao, Z. P. *et al.* Piezoelectric and dielectric properties of Ce substituted  $\text{La}_2\text{Ti}_2\text{O}_7$  ceramics. *J. Euro. Ceram. Soc.* **33**, 1001–1008, (2013).
21. Lichtenberg, F., Herrnberger, A. & Wiedenmann, K. Synthesis, structural, magnetic and transport properties of layered perovskite-related titanates, niobates and tantalates of the type  $\text{A}_n\text{B}_n\text{O}_{(3n+2)}$ ,  $\text{A}'\text{A}_{(k-1)}\text{B}_k\text{O}_{(3k+1)}$  and  $\text{A}_m\text{B}_{(m-1)}\text{O}_{3m}$ . *Prog. Solid State. Ch.* **36**, 253–387 (2008).
22. Yan, H., Ning, H., Kan, Y., Wang, P. & Reece, M. J. Piezoelectric ceramics with super-high curie points. *J. Am. Ceram. Soc.* **92**, 2270–2275 (2009).
23. Gomah-Petry, J. R., Sai, S., Marchet, P. & Mercurio, J. P. Sodium-bismuth titanate based lead-free ferroelectric materials. *J. Euro. Ceram. Soc.* **24**, 1165–1169 (2004).
24. Donaji, Y., Suarez, I. M. & Lee, W. E. Relation between tolerance factor and  $T_c$  in Aurivillius compounds. *J. Mater. Res.* **16**, 3139–3149 (2001).
25. Scheunemann, K. & Mullerbuschbaum, H. Crystal-structure of  $\text{Nd}_2\text{Ti}_2\text{O}_7$ . *J. Inorg. Nucl. Chem.* **37**, 2261–2263 (1975).
26. Ishizawa, N., Marumo, F., Kawamura, T. & Kimura, M. Crystal-structure of  $\text{Sr}_2\text{Nb}_2\text{O}_7$ , a compound with perovskite-type slabs. *Acta Crystallogr. B* **31**, 1912–1915 (1975).
27. Ishizawa, N., Marumo, F., Kawamura, T. & Kimura, M. Compounds with perovskite-type slabs. II. crystal-structure of  $\text{Sr}_2\text{Ta}_2\text{O}_7$ . *Acta Crystallogr. B* **32**, 2564–2566, (1976).
28. Ishizawa, N., Marumo, F., Iwai, S., Kimura, M. & Kawamura, T. Compounds with perovskite-type slabs. V. A high-temperature modification of  $\text{La}_2\text{Ti}_2\text{O}_7$ . *Acta Crystallogr. B* **38**, 368–372 (1982).
29. Ishizawa, N., Ninomiya, K., Sakakurab, T. & Wang, J. Redetermination of  $\text{Nd}_2\text{Ti}_2\text{O}_7$ : a noncentrosymmetric structure with perovskite-type slabs. *Acta Crystall. Sec. E* **69**, 119 (2013).
30. Pöykkö, S. & Chadi, D. J. Ab initio study of dipolar defects and  $180^\circ$  domain walls in  $\text{PbTiO}_3$ . *J. Phys. Chem. Solids* **61**, 4 (2000).
31. Jaffe, B., Cook, W. & Jaffe, H. In Non-metallic solids, *Piezoelectric Ceramics*. Vol. 3 317 (University of Michigan, 1971).
32. Shimakawa, Y. *et al.* Crystal structure and ferroelectric properties of  $\text{ABi}_2\text{Ta}_2\text{O}_9$  (A = Ca, Sr, and Ba). *Phys. Rev. B.* **61**, 6559–6564 (2000).
33. Lichtenberg, F., Herrnberger, A., Wiedenmann, K. & Mannhart, J. Synthesis of perovskite-related layered  $\text{A}_n\text{B}_n\text{O}_{(3n+2)} = \text{ABO}_x$  type niobates and titanates and study of their structural, electric and magnetic properties. *Prog. Solid State. Ch.* **29**, 1–70 (2001).

## Acknowledgements

This presented work is partly supported by the CSS project with grant No. YK2015-0602006. Dr. Zhipeng Gao would acknowledge the treatments from Prof. Mike Reece and Dr. Haixue Yan at Queen Mary, University of London.

## Author Contributions

Z.G. conceived the idea. Z.G. and C.L. wrote the main manuscript text. Y.W. and S.Y. prepared Figures 1–3. Y.Y. and H.H. prepared the Figures 4–5.

## Additional Information

**Competing financial interests:** The authors declare no competing financial interests.

**How to cite this article:** Gao, Z. *et al.* Super Stable Ferroelectrics with High Curie Point. *Sci. Rep.* **6**, 24139; doi: 10.1038/srep24139 (2016).



This work is licensed under a Creative Commons Attribution 4.0 International License. The images or other third party material in this article are included in the article's Creative Commons license, unless indicated otherwise in the credit line; if the material is not included under the Creative Commons license, users will need to obtain permission from the license holder to reproduce the material. To view a copy of this license, visit <http://creativecommons.org/licenses/by/4.0/>